PNAS RESEARCH ARTICLE | IMMUNOLOGY AND INFLAMMATION

Stem cell decoupling underlies impaired lymphoid development during aging

Geunhyo Jang[a,1], Stephania Contreras Castillo[b,1], Eduardo Esteva[a,c], Samik Upadhaya[a], Jue Feng[a], Nicholas M. Adams[a], Elodie Richard[b], Rajeshwar Awatramani[d], Catherine M. Sawai[b,2], and Boris Reizis[a,2]

Edited by Ellen Rothenberg, California Institute of Technology, Pasadena, CA; received February 7, 2023; accepted April 20, 2023

Mammalian aging is associated with multiple defects of hematopoiesis, most prominently with the impaired development of T and B lymphocytes. This defect is thought to originate in hematopoietic stem cells (HSCs) of the bone marrow, specifically due to the age-dependent accumulation of HSCs with preferential megakaryocytic and/or myeloid potential ("myeloid bias"). Here, we tested this notion using inducible genetic labeling and tracing of HSCs in unmanipulated animals. We found that the endogenous HSC population in old mice shows reduced differentiation into all lineages including lymphoid, myeloid, and megakaryocytic. Single-cell RNA sequencing and immunophenotyping (CITE-Seq) showed that HSC progeny in old animals comprised balanced lineage spectrum including lymphoid progenitors. Lineage tracing using the aging-induced HSC marker *Aldh1a1* confirmed the low contribution of old HSCs across all lineages. Competitive transplantations of total bone marrow cells with genetically marked HSCs revealed that the contribution of old HSCs was reduced, but compensated by other donor cells in myeloid cells but not in lymphocytes. Thus, the HSC population in old animals becomes globally decoupled from hematopoiesis, which cannot be compensated in lymphoid lineages. We propose that this partially compensated decoupling, rather than myeloid bias, is the primary cause of the selective impairment of lymphopoiesis in older mice.

aging | lymphopoiesis | hematopoietic stem cells

Significance

The development of T and B lymphocytes, which mediate immune responses to infections and vaccines, is impaired in the old age. This defect originates in hematopoietic stem cells (HSCs) that give rise to all blood cell lineages including lymphocytes, but the underlying mechanism remains unclear. Here, we traced the contribution of HSCs to blood development in unmanipulated old mice and found it to be reduced across all lineages. This global reduction, herein termed decoupling, appears to be compensated in some lineages but not in T cell development, leading to the selective impairment of the latter. The results help explain the salient feature of mammalian aging and have implications for rejuvenation of the immune system in older mice.

During the lifetime of an organism, the immune system undergoes profound changes that contribute to and exacerbate the aging process (1). Thus, children and young adults manifest extensive lymphoid development that builds the repertoire of long-lived T and B lymphocytes. This wave of lymphopoiesis declines over time along with the involution of the thymus, which likely contributes to the decline. Conversely, hematopoiesis in aging individuals shows a shift toward myeloid differentiation, as myeloid cells such as monocytes and granulocytes are short-lived and require constant production. This age-related shift prevents the replenishment of peripheral lymphocytes, thereby contributing to immunodeficiency in the elderly and precluding the regeneration of the lymphoid compartment, for instance after transplantation (2). It is also thought to lead to a predisposition to myeloproliferative disorders and myeloid leukemia, the incidence of which increases steadily with age (3).

Age-associated defects of immune development are thought to originate in hematopoietic stem cells (HSCs), the small self-renewing population in the adult bone marrow (BM) that sustains hematopoiesis throughout adult life (4, 5). Indeed, HSCs in old animals are increased in numbers and manifest abnormalities in gene expression, cell cycle control, polarity, and DNA damage response (6). To explain the age-dependent decline of lymphopoiesis, it is generally thought that the HSC population in old mammals acquires a "myeloid bias." Indeed, HSCs were shown to comprise several types that differ in their lineage potential and self-renewal capacity (7–11). It has been shown that the accumulation of HSCs with preferential myeloid and/or megakaryocytic potential skews blood production toward these lineages at the expense of lymphocytes in old animals (12–18). However, this model has been based predominantly on the transplantation of isolated HSCs, which does not take into account the expanded HSC population. Moreover, HSCs with lymphoid potential were recently reported to be intact in old animals (19), and the reconstitution capacity of the total BM from old animals (as opposed to isolated HSCs) is not impaired (14, 20). Thus, the mechanism of the selective lymphopoiesis defect in old mammals is unclear and remains to be tested in the context of endogenous hematopoiesis.

Here, we used inducible lineage tracing of endogenous HSCs to assess the source and mechanism of impaired lymphopoiesis in unmanipulated old animals. Surprisingly, we found no prominent lineage bias in the old HSC population; instead, its differentiation was reduced across all lineages, revealing a global decoupling of the HSC population from

Author contributions: G.J., S.C.C., S.U., J.F., C.M.S., and B.R. designed research; G.J., S.C.C., S.U., J.F., N.M.A., and E.R. performed research; R.A. contributed new reagents/analytic tools; G.J., S.C.C., E.E., J.F., C.M.S., and B.R. analyzed data; and G.J., S.C.C., C.M.S., and B.R. wrote the paper.

The authors declare no competing interest.

This article is a PNAS Direct Submission.

[1]G.J. and S.C.C. contributed equally to this work.

[2]To whom correspondence may be addressed. Email: catherine.sawai@u-bordeaux.fr or boris.reizis@nyulangone.org.

This article contains supporting information online at https://www.pnas.org/lookup/suppl/doi:10.1073/pnas.2302019120/-/DCSupplemental.

Published May 22, 2023.

hematopoiesis. By combining HSC tracing with competitive BM transplantation, we found that HSC decoupling could not be compensated in lymphocytes and particularly in T cells, suggesting a mechanism for the selective impairment of T cell development in old age.

Results

Global Reduction of HSC Differentiation in Old Animals. Previously, we generated a mouse strain in which a tamoxifen-regulated Cre recombinase is expressed from an HSC-specific transgene (*Pdzk1ip1*-CreER). When combined with Cre-inducible fluorescent reporters such as *Rosa26*-LoxStopLox-tdTomato ($R26^{Tom}$), this strain allows tamoxifen-inducible labeling of adult HSCs and tracing of their progeny. The results revealed a major sustained contribution of HSCs to hematopoiesis in adult mice; notably, however, the labeling of lymphocytes remained lower than that of myeloid cells after 6 to 9 mo (21). We tested HSC contribution over the entire lifespan by inducing HSC labeling in young *Pdzk1ip1*-CreER $R26^{Tom/Tom}$ reporter mice and tracing the fraction of tdTomato (Tom)-positive labeled cells in the peripheral blood (PB) and in the BM and spleen at the end point. Reporter mice were induced with tamoxifen at 2 mo of age and traced for ~21 mo thereafter (Fig. 1*A*). The fraction of Tom^+-labeled myeloid cells reached the plateau of ~80% at 15 mo., whereas labeled B cells progressively accumulated to a comparable frequency by 21 mo. In contrast, T cell labeling reached ~50% at 12 mo and remained constant thereafter, significantly below the labeling of myeloid cells (Fig. 1*B*). End point analysis showed a comparable ~80% labeling of HSCs, downstream progenitors and myeloid cells, and B cells, whereas the labeling of T cells was reduced, presumably due to the well-established longevity of the peripheral T cell pool (Fig. 1 *C* and *D*). These data suggest that HSCs equilibrate with their progeny during the lifespan and give rise to nearly all myeloid cells and B cells in old animals.

To test the contribution of HSCs to blood lineages specifically in old animals, we induced old or control young adult *Pdzk1ip1*-CreER $R26^{Tom/Tom}$ reporter mice with tamoxifen and performed BM biopsy at 3 d to analyze Tom expression in HSCs. The efficiency and specificity of Tom labeling in old mice were comparable to those in young mice (*SI Appendix*, Fig. S1 *A* and *B*). However, the analysis of the same mice after 4 wk revealed a reduced accrual of Tom^+ cells in MPP3/4, EryP, and particularly in MyP in old mice (*SI Appendix*, Fig. S1*C*), suggesting that HSC differentiation was reduced. To test long-term HSC differentiation, we similarly labeled HSCs in old or young adult mice and traced them for 6 mo (Fig. 1*E*). The accrual of HSC-derived mature Tom^+ cells was reduced ~twofold in all blood lineages including platelets, myeloid cells, B lymphocytes, and NK cells (Fig. 1*F*). An even stronger ~fivefold reduction was observed in T cells, again likely reflecting the stability of the peripheral T cell pool in old animals. End point analysis at 26 mo revealed reduced labeling of myeloid and lymphoid cells in the BM (Fig. 1*G*) and of all cell subsets in the thymus, including early thymic progenitors (ETP), $CD4^-CD8^-$ double-negative (DN2-DN4), $CD4^+CD8^+$ double-positive (DP), and $CD4^+$ or $CD8^+$ single-positive thymocytes (Fig. 1*H*). The result was confirmed in an independent tracing experiment, in which the initial labeling efficiency was not significantly different between young and old HSCs, but the long-term output of the latter was significantly reduced in all lineages (*SI Appendix*, Fig. S2).

The fraction of labeled HSCs at the end point reached ~80% in control adult mice (Fig. 1*I*), reflecting the differentiation of originally labeled "top-level" HSCs into downstream HSCs as described (21). Accordingly, the end point frequency of Tom^+ HSCs and of all downstream progenitors was significantly decreased in old mice (Fig. 1*I*). However, given the expansion of HSC numbers in old mice (Fig. 1*J*), the number of labeled HSCs in old mice was still increased threefold compared to controls, while the numbers of labeled downstream populations including ST-HSC were significantly decreased (Fig. 1*K*). Thus, although the HSC population in old mice is expanded, its net contribution is reduced in all hematopoietic lineages, suggesting a global differentiation defect.

To test whether the observed defect of HSC differentiation is unique to aging, young *Pdzk1ip1*-CreER $R26^{Tom/Tom}$ were treated with: i) sublethal irradiation, which causes acute ablation of leukocytes followed by recovery by ~8 wk; ii) the double-stranded RNA polymer poly-I:C, which induces acute type I interferon (IFN-α/β, IFN-I) response that activates HSC proliferation but ultimately leads to their exhaustion (22–24); iii) adenoviral vector encoding IFN-a (IFNa-Adv), which induces systemic production of IFN-a by hepatocytes for several weeks (25). Four, seven, or ten weeks after poly-I:C, irradiation, or IFNa-Adv, respectively, mice were treated with tamoxifen to induce HSC labeling, tested by BM biopsy, and monitored for up to 32 wk (*SI Appendix*, Fig. S3*A*). The efficiency and specificity of HSC labeling were comparable between all treated and control mice (*SI Appendix*, Fig. S3*B*). Tracing of Tom^+ HSC progeny over time in the PB and at the end point in the BM showed that the labeling of all lineages was comparable between stress-treated and control mice (*SI Appendix*, Fig. S3 *C–E*). Thus, prior exposure to acute (irradiation, poly-I:C) or chronic (IFNa-Adv) hematopoietic stress had no major impact on HSC differentiation, suggesting that its global reduction is specific for the aging process.

Normal Differentiation Spectrum of Old HSCs In Vivo. We examined the early steps of HSC differentiation by combining lineage tracing with single-cell transcriptomics using Cellular Indexing of Transcriptomes and Epitopes by Sequencing (CITE-Seq). CITE-Seq enables combined single-cell RNA sequencing, cell surface marker detection using antibody-derived tags (ADT) (26), and labeling of individual samples using antibody "hashtags" (27). We labeled HSCs in vivo by inducing old or young *Pdzk1ip1*-CreER $R26^{Tom/Tom}$ reporter mice with tamoxifen, and 4 wk later, we isolated Lineage-negative (Lin^-) BM cells from individual mice (n = 3 per age group). Cells from each animal were labeled with ADT and animal-specific hashtags. Tom^+ HSCs and their progeny within the Lin^- $c\text{-}Kit^+$ population were sorted, and the resulting cells were mixed in equivalent numbers and analyzed by CITE-Seq. Clustering analysis of the resulting 9,635 cells resulted in 14 clusters visualized in a uniform manifold approximation and projection (UMAP) plot in two dimensions (Fig. 2*B*). To assign cluster identities, the expression signature of each cluster was compared to that of reference datasets (*SI Appendix*, *Methods*) and supported by curated analysis of top gene and ADT markers associated with HSCs, progenitor, and lineage-committed cells (Fig. 2*C*). This approach resulted in the identification of HSCs at the apex of the UMAP plot (here designated LT-HSC for concordance with reference datasets), followed below by i) megakaryocyte-primed progenitors (MPP2, MkP, and cycling MkP); ii) multipotent progenitors (ST-HSC, MPP3, and MPP4); iii) erythroid progenitors (EryP, pre-CFU-E, and CFU-E); and iv) myeloid progenitors (GMP, MDP, basophil/mast cell progenitor, and a small cluster of DC progenitors).

The HSC cluster was comprised predominantly (90%) of HSCs from the old animals; the ST-HSC and MPP2 clusters were also enriched in respective cells from the old animals, albeit to a lower degree (71% and 75%, respectively) (Fig. 2*D*). In contrast, more

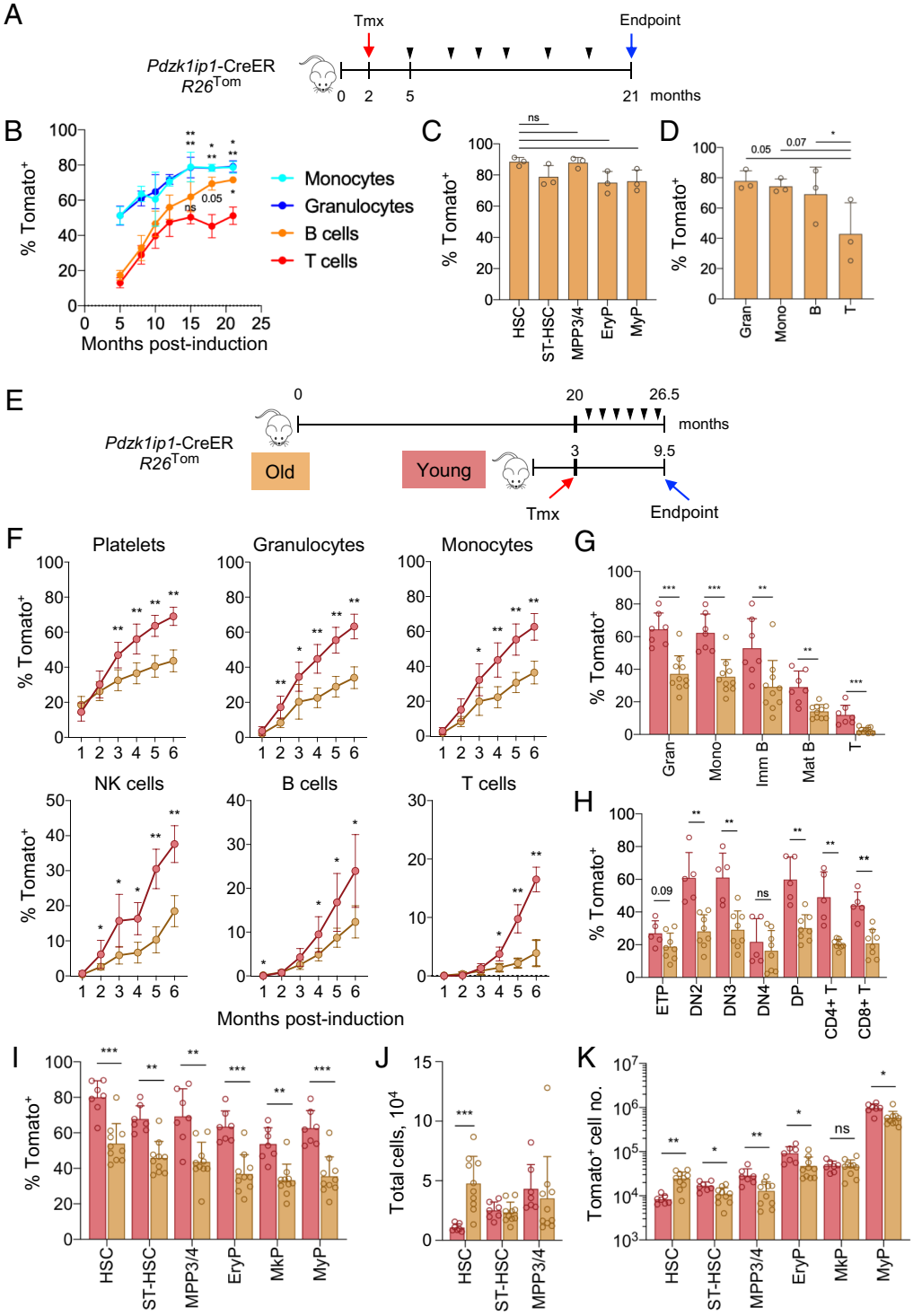

Fig. 1. Reduced contribution of endogenous HSCs to hematopoiesis in old animals. (*A*) Labeling and tracing of young HSCs across the lifespan. *Pdzk1ip1*-CreER transgenic mice were crossed with the Cre-inducible *Rosa26*-StopFlox-tdTomato (*R26*^{Tom}) fluorescent reporter. Young adult mice were administered tamoxifen to induce Tom expression in HSCs and monitored for Tom expression in PB starting at 5 mo of age (arrowheads), followed by end point analysis at 21 mo. (*B*) The fraction of labeled Tom$^+$ cells in major blood cell types over the lifespan after tamoxifen treatment (mean ± SD of 4 mice). Significance of differences between T cells and granulocytes (*Top*), monocytes (*Middle*), and B cells (*Bottom*) is indicated. (*C* and *D*) Fractions of Tom$^+$ HSC and progenitors (*C*) and mature cell types (*D*) in the BM at the end point. Symbols represent individual mice; bars represent mean ± SD; significance of differences between T cells and other cell types in panel *E* is indicated. (*E*) Labeling and long-term tracing of HSCs in old animals. Old or young adult *Pdzk1ip1*-CreER *R26*$^{Tom/Tom}$ mice were treated with Tmx, bled monthly, and analyzed at the endpoint. (*F*) Cell labeling in the peripheral blood of induced reporter animals. Shown are fractions of Tom$^+$ cells within the indicated cell type in young or old reporter mice at the indicated time points after tamoxifen induction. Symbols represent mean ± SD of 7 old or 4 young mice. (*G*–*K*) The analysis of young (salmon) or old (orange) reporter animals at the endpoint. Symbols represent individual mice; bars represent mean ± SD; data are pooled from two independent experiments. (*G*–*I*) Fractions of labeled Tom$^+$ cells among mature BM cells (*G*), thymocyte subsets (*H*), and HSC/progenitor cells in the BM (*I*). (*H* and *I*) Absolute numbers of total (*H*) and labeled Tom$^+$ (*I*) HSC/progenitor cells in the BM. Statistical significance was estimated by Mann–Whitney *U* test. *$P < 0.05$; **$P < 0.01$; ***$P < 0.001$; ns, not significant.

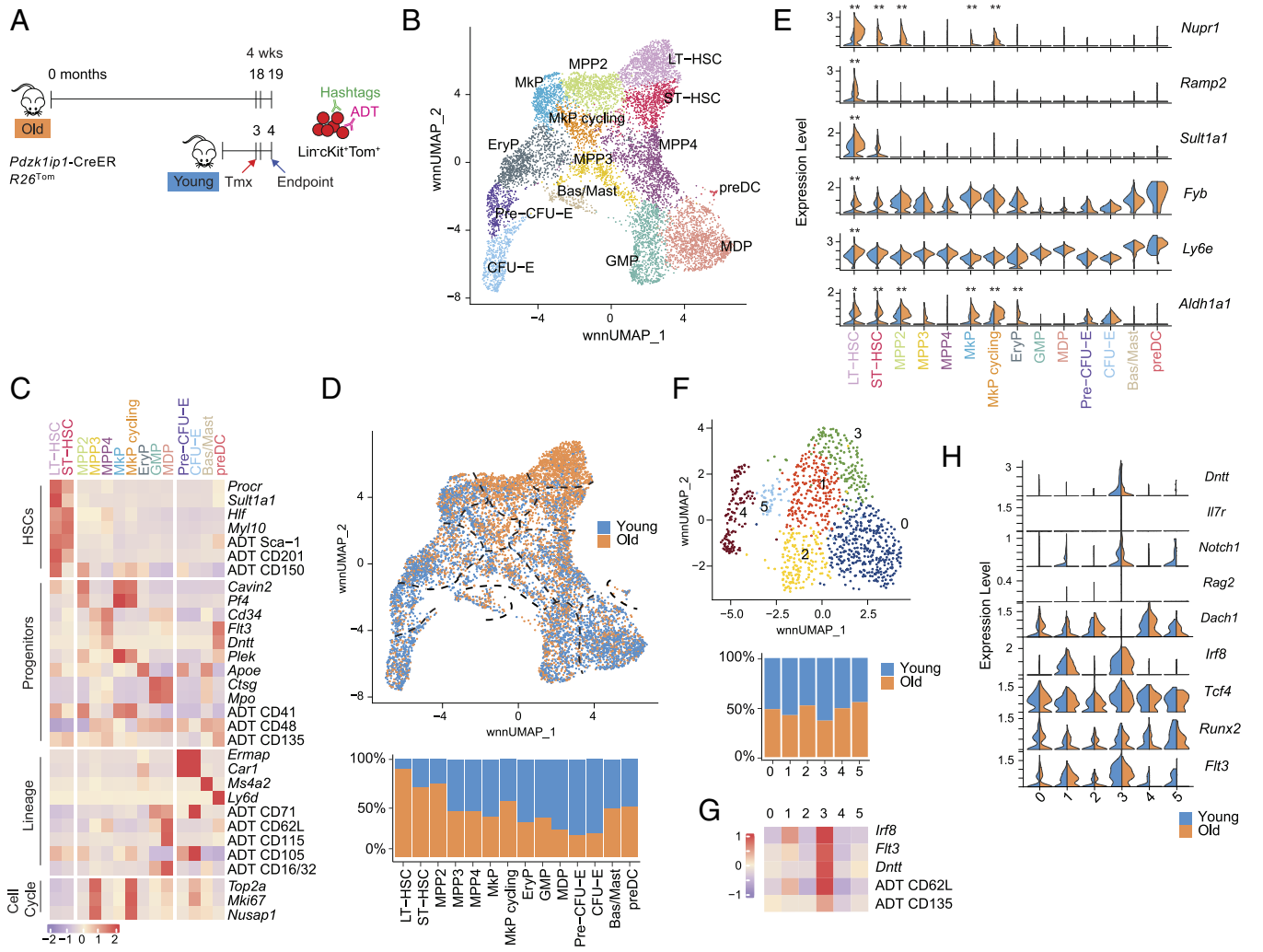

Fig. 2. Balanced lineage output of HSCs in old animals. (*A*) Experimental setup of single-cell transcriptomic and immunophenotypic analysis of labeled HSCs and their early progeny. Young or old *Pdzk1ip1*-CreER *R26*$^{Tom/Tom}$ mice were treated with Tmx; 4 wk later, Lineage$^-$ cKit$^+$ Tom$^+$ BM cells were isolated separately from three individual mice per condition, hashtagged, pooled, and analyzed by CITE-Seq. (*B*) UMAP plot of single cells clustered by transcriptomic and phenotypic data. Resulting clusters are indicated by color and labeled with their proposed identity. (*C*) Heatmap of average expression levels of transcripts for HSC, progenitor, lineage, and cell cycle–associated markers. ADT expression is indicated for some surface markers. Expression values were linearly interpolated between −2 and 2. Note that the cell cycle–associated gene expression signature has been regressed during the analysis, resulting in a relative reduction of cell cycle–associated transcripts in proliferative clusters such as MPP4 and pre-CFU-E. (*D*) The distribution of old and young cells within the clusters. Shown is the UMAP plot of single cells colored by condition, and bar plot shows the percentage of their contribution to each cluster. (*E*) Aging signature genes that showed significant differential expression between old and young HSCs. Shown are split violin plots of transcript expression values per condition across the clusters. Significance is indicated as follows: **P.val* < 0.001; ***P.adj* < 0.001. (*F*) Reclustering of the MPP4 cluster to reveal additional heterogeneity. Shown is the UMAP plot of MPP4 with clusters indicated by color, and bar plot shows the fraction of young vs. old cells per cluster. (*G*) Heatmap of the average expression of genes and ADTs associated with lymphoid or DC progenitors. Expression values were linearly interpolated between −2 and 2. (*H*) Split violin plot of the transcript expression values per condition for genes associated with lymphoid or pDC development.

differentiated cell clusters contained equal (e.g., MPP4, MkP) or reduced (e.g., CFU-E) fractions of respective cells from old mice, consistent with the specific expansion of the HSC compartment in old mice. We then defined differentially expressed genes between old and young cells within each cluster and compared them to the consensus Aging Signature (AS) of old murine HSCs (28). Six out of the 20 AS genes defined as "best aging predictors" were significantly enriched in old HSCs (Fig. 2*E*), revealing both the expected numerical expansion and the aging-associated expression signature of old HSCs. In contrast, old cells in downstream progenitors were either represented equally (e.g., MPP3, MPP4, MkP) or were slightly reduced (e.g., in pre-CFU-E and CFU-E) compared to young cells (Fig. 2*D*). Although no distinct lymphoid cluster was present at this early stage as expected (29), we noticed weak expression of the lymphoid marker *Dntt* in the MPP4 population (Fig. 2*C*). We reclustered MPP4 (Fig. 2*F*) and identified a distinct subcluster (#3) that was enriched for surface markers Flt3 (CD135) and CD62L and lymphoid-associated transcripts *Dntt, Flt3,* and *Notch1* (Fig. 2*G*). This population did not express transcripts associated with advanced lymphoid differentiation such as *Il7r* or *Rag2* yet was specifically negative for *Dach1* (Fig. 2*H*), and thus was overall consistent with the earliest lymphoid progenitor within MPP (30–32). Critically, the progeny of old and young HSCs was represented equally in this population and all other MPP4 subclusters (Fig. 2*F*), suggesting normal lymphoid differentiation of old HSCs.

We next specifically focused on lymphoid progeny of HSCs by using CITE-Seq at 8 wk after tamoxifen-induced HSC labeling, when lymphoid differentiation of HSCs has commenced (29). We sorted Tom-labeled BM cells that were Lin$^-$ Flt3$^+$, thereby excluding HSCs and their numerous erythromyeloid progeny, but including the progenitors of lymphocytes and DCs (Fig. 3*A*). As

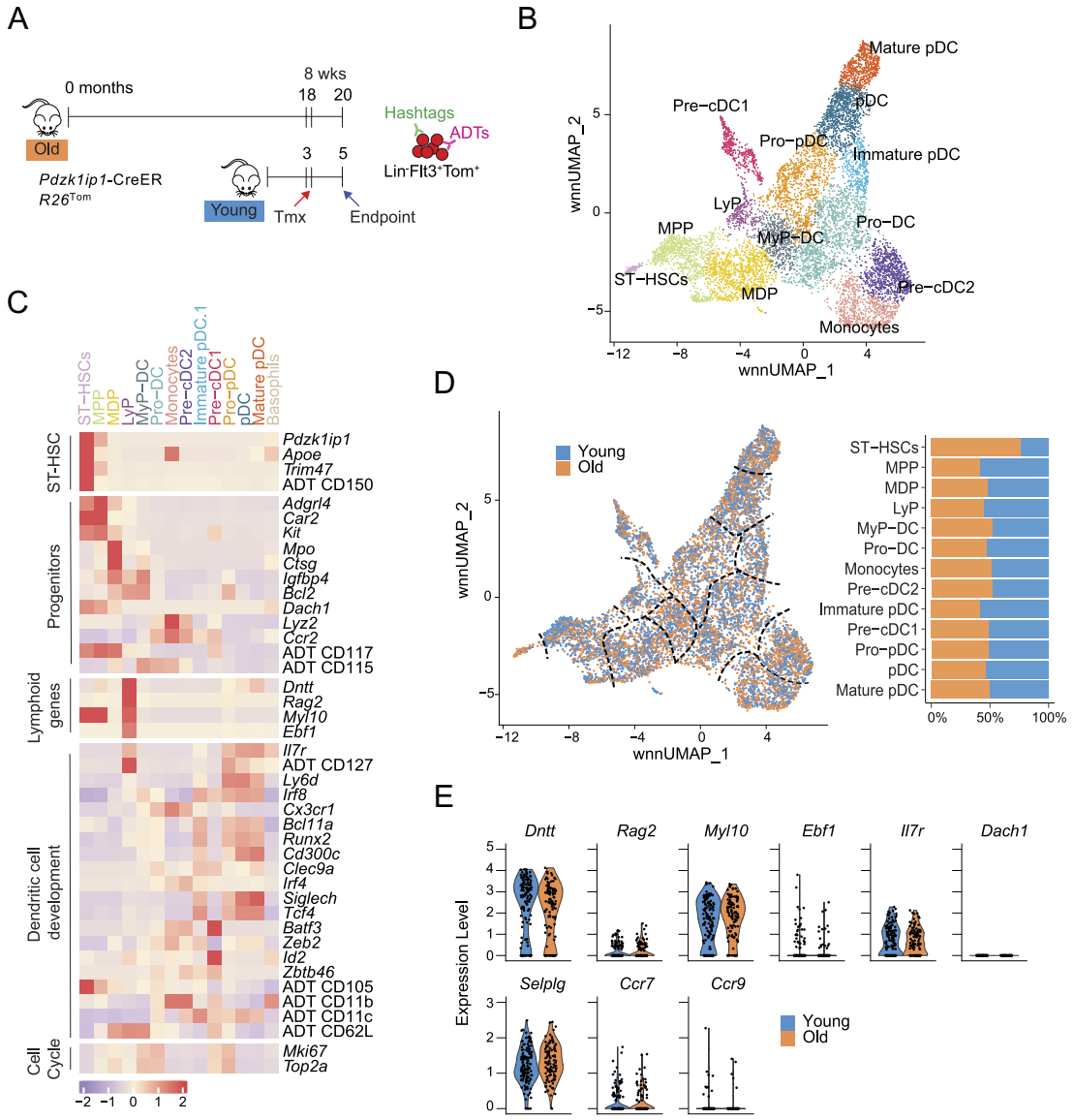

Fig. 3. Normal lymphoid differentiation of HSCs in old animals. (*A*) Experimental setup of single-cell transcriptomic and immunophenotypic analysis of lymphoid differentiation. Young or old *Pdzk1ip1*-CreER *R26*$^{Tom/Tom}$ mice were treated with Tmx; 8 wk later, Lineage$^-$ Flt3$^+$ Tom$^+$ BM cells were isolated separately from three individual mice per condition, hashtagged, pooled, and analyzed by CITE-Seq. (*B*) UMAP plot of single cells clustered by transcriptomic and phenotypic data. Resulting clusters are indicated by color. A small contaminating population of basophils was excluded from the plot. (*C*) Heatmap of the mean expression of transcripts and phenotypic markers for HSC, progenitors, lymphoid, dendritic cell development, and cell cycle–associated markers. Expression values were linearly interpolated between −2 and 2. (*D*) The distribution of old and young cells within the clusters. Shown is the UMAP plot of single cells colored by condition, and bar plot shows the percentage of their contribution to each cluster. (*E*) Violin plots of the transcript expression values of lymphoid-associated genes in the LyP cluster colored by condition.

in the first experiment, ADT- and hashtag-labeled cells from each animal were sorted, mixed in equivalent numbers, and analyzed by CITE-Seq. After quality control, 8,986 cells derived from independent young or old animals (n = 3 per age group) were analyzed as above, yielding 14 clusters. Apart from a single outlier cluster of basophil-like cells, the remaining 13 clusters comprised the expected Flt3$^+$ populations including ST-HSC, MPP, and multiple DC progenitors corresponding to the recently described hierarchy of DC differentiation (33) (Fig. 3 *B* and *C*). ST-HSCs were enriched in old cells, consistent with the results obtained at 4 wk (Fig. 2*B*), whereas all other clusters were composed of old and young cells in equal proportions (Fig. 3*D*). In contrast to the 4-wk timepoint, the HSC progeny at 8 wk included a distinct cluster of LyP that expressed the *Il7r* transcript and surface IL-7R (CD127), as well as canonical lymphoid transcripts *Dntt*, *Rag2*, *Myl10,* and *Ebf1* (Fig. 3*C*). Importantly, old and young cells were represented equally in this cluster (Fig. 3*D*) and expressed similar levels of transcripts associated with lymphoid development (see above) and with migration to the thymus such as *Selplg*, *Ccr9,* and *Ccr7* (34, 35) (Fig. 3*E*). Collectively, unbiased single-cell analysis at two time points suggests that the progeny of old HSCs is reduced relative to the size of the HSC compartment, but comprises a balanced spectrum of differentiation to all lineages including lymphocytes.

Reduced Differentiation of Old HSCs Revealed by Aging-Specific Tracing. To further characterize the old HSC compartment at the single-cell level, we reexamined HSCs that were identified in the 4-wk CITE-Seq analysis, comprising 104 cells from young and 981 cells from old mice. Reclustering using transcriptomic and phenotypic data yielded four clusters that were relatively poorly resolved on the UMAP plot (*SI Appendix*, Fig. S4*A*). All

clusters were dominated by the more numerous old HSCs but nevertheless consisted of cells from both conditions (*SI Appendix*, Fig. S4 *B–E*). Notably, all up-regulated best aging predictor genes (Fig. 2*E*) were up-regulated in all the four clusters compared to young HSCs (*SI Appendix*, Fig. S4*F*). Conversely, genes specific for megakaryocytic (*Vwf*, *Selp*, *Pf4*, *Itga2b,* and *Fhl1*) or myeloid (*Mpo*, *Csf1r*, *Csf2ra*, *Ms4a6b*, *Csf3r*, and *Spi1*) development did not show a significant enrichment in any cluster of old HSCs (*SI Appendix*, Fig. S4 *G* and *H*). To further explore the potential heterogeneity of the old HSC population, we interrogated it by single-cell Assay for Transposase-Accessible Chromatin sequencing (scATAC-Seq). The resulting clusters were compared to bulk ATAC-Seq profiles of murine immune cells (36), and clusters corresponding to cells other than HSCs were iteratively removed. The remaining HSC population comprised four closely affiliated clusters and was relatively homogeneous (*SI Appendix*, Fig. S4*I*), in an agreement with a recent scATAC-Seq analysis of murine HSCs (37). This publication described differentially accessible chromatin regions (DARs) that became more accessible (opened) or less accessible (closed) specifically in old HSCs; some of the opened DARs corresponded to genes up-regulated in old HSCs such as *Cavin2* (*Sdpr*) and *Aldh1a1*. We found that both opened and closed DARs defined by Itokawa et al. were distributed evenly across the old HSC population (*SI Appendix*, Fig. S4*J*), including DARs in *Cavin2* and *Aldh1a1* (*SI Appendix*, Fig. S4*K*). Collectively, these data suggest that age-associated transcriptional and epigenetic features are acquired by the entire HSC population in old animals.

Aldh1a1, encoding a member of the aldehyde dehydrogenase family, is up-regulated in old HSCs (38, 39) and is one of the best aging predictor genes in the aging signature of these cells (28). Our above-described analysis of the old HSC population confirmed the prominent upregulation of *Aldh1a1* and suggested that it was occurring across the entire HSC population rather than in a specific subset. We therefore used mice with CreER inserted into the endogenous *Aldh1a1* locus (40) to specifically label and trace HSCs in old mice. Old (18 mo) or young adult (3 mo) *Aldh1a1*^{CreER} *R26*$^{Tom/Tom}$ were administered a single dose of tamoxifen followed by BM biopsy after 3 d, monthly tracing in the PB, and endpoint analysis 5.5 mo later (Fig. 4*A*). We found that young mice showed minimal (0 to 4%) labeling of HSCs and progenitors, whereas old mice harbored ~30% of labeled Tom$^+$ HSCs compared to <5% of labeled ST-HSCs and progenitors (Fig. 4*B*). Accordingly, subsequent Tom labeling in the PB of young mice was minimal (<3%) in platelets and myeloid cells and virtually undetectable in B and T cells (Fig. 4*C*). Old mice, on the contrary, showed progressive label accrual, revealing the long-term multilineage contribution of *Aldh1a1*$^+$ HSCs to hematopoiesis. However, by 5 mo postinduction, the labeling reached only ~23% in platelets, ~12% in myeloid cells, and <1% in B and T cells (Fig. 4*C*), as confirmed at the end point (Fig. 4*D*). Accordingly, the end point analysis showed ~40% labeling of HSCs vs. ~10% of MPP and <5% of all progenitors including MkP and MyP (Fig. 4*E*). The ETP in the thymus was labeled at equally low levels, whereas the labeling of subsequent thymocyte stages was virtually absent in two out of three animals (Fig. 4*F*). Overall, induced *Aldh1a1*^{CreER} reporter mice showed low rate of labeling in all lineages, even by comparison to old *Pdzk1ip1*-CreER reporter animals at the same time point (Fig. 4*G*). This is likely because *Aldh1a1*^{CreER} labels a random sample of the HSC population rather than the top-level HSCs labeled by *Pdzk1ip1*-CreER. Thus, old HSCs marked by the expression of *Aldh1a1* sustain their own population but show a low differentiation rate across the entire lineage spectrum.

Reduced HSC Activity in Old Animals Is Not Compensated in Lymphocytes. To reconcile the observed multilineage reduction of HSC differentiation with the specific impairment of lymphopoiesis in old mice, we used transplantation of the total BM in which HSCs and their progeny can be specifically traced. We induced HSC labeling with tamoxifen in old (20 mo) or young adult (3 mo) *Pdzk1ip1*-CreER *R26*$^{Tom/Tom}$ reporter mice, isolated total BM cells shortly after labeling, and transferred them into irradiated young CD45.1 congenic recipients along with competitor BM cells from young CD45.1 congenic mice (Fig. 5*A*). Approximately half of the HSCs were Tom$^+$ in the BM from old and young donors, although the absolute HSC numbers were increased ~fourfold in the former (Fig. 5*B*). Donor-derived platelets in this experiment could not be traced with confidence due to their lack of CD45 expression. In this experiment, even the young BM showed lower donor reconstitution in lymphoid (<30%) compared to myeloid (~55%) cells (Fig. 5*C*). This was observed previously (29) and may reflect the short-term effect of tamoxifen on the lymphoid reconstitution capacity, as tamoxifen may engage the estrogen receptor (41) that inhibits lymphopoiesis (42). The overall donor reconstitution (i.e., both Tom$^+$ and Tom$^-$ CD45.2$^+$ cells, total shaded areas in Fig. 5*C*) in myeloid cells was comparable between the old and young BM. HSC-derived Tom$^+$ cells accounted for nearly all myeloid cells derived from the young BM, consistent with the high reconstitution capacity of labeled HSCs (29). In contrast, a large fraction of myeloid cells derived from the old BM was Tom$^-$, suggesting a compensation from unlabeled HSCs or progenitors. Both total and Tom$^+$ T cells derived from the old BM were reduced, suggesting that the defective T cell reconstitution by old HSCs cannot be compensated.

At the 6-mo end point, the vast majority of CD45.2$^+$ donor–derived mature cells, HSCs, and progenitors were Tom$^+$ in all recipient groups (Fig. 5 *D* and *E* and *SI Appendix*, Fig. S5*A*). The progeny of Tom$^+$ HSCs was only slightly decreased in the recipients of old BM compared to the young BM; however, the contribution of Tom$^-$ cells was significantly increased in myeloid progenitors and mature cells. In contrast, thymocytes showed a drastically reduced contribution of Tom$^+$ HSCs that was not compensated by Tom$^-$ cells (Fig. 5*F*). When the fractions of Tom$^+$ cells were normalized by the number of transferred Tom$^+$ HSCs (Fig. 5*B*), the contribution of labeled HSCs in the old donor BM was significantly reduced in myeloid cells (~fivefold), B cells (~sevenfold), and T cells (20-fold) (*SI Appendix*, Fig. S5*B*). On the contrary, the normalized fractions of old Tom$^-$ cells were normal in myeloid cells but showed a significant >threefold reduction in T and B lymphocytes (*SI Appendix*, Fig. S5*B*). Collectively, our data suggest that the HSC population in the BM of old mice, although expanded in numbers, shows reduced contribution to hematopoiesis both in native hosts and upon transplantation. We hereby term this phenomenon "decoupling," to emphasize the global dissociation between stem cell activity and final stages of mature blood cell production, irrespectively of any potential lineage biases within the HSC population. This decoupling may be compensated by other cellular sources to maintain normal output of myeloid cells but not of lymphocytes, particularly of T cells.

Discussion

Multiple inducible lineage-tracing experiments in young adult mice (21, 43–45) have shown that major hematopoietic cell populations including platelets, granulocytes, monocytes, and lymphocytes (T, B, and NK cells) are continuously generated from HSCs in adult animals. Here, we further demonstrate that nearly all myeloid cells and B cells are generated from HSCs over the

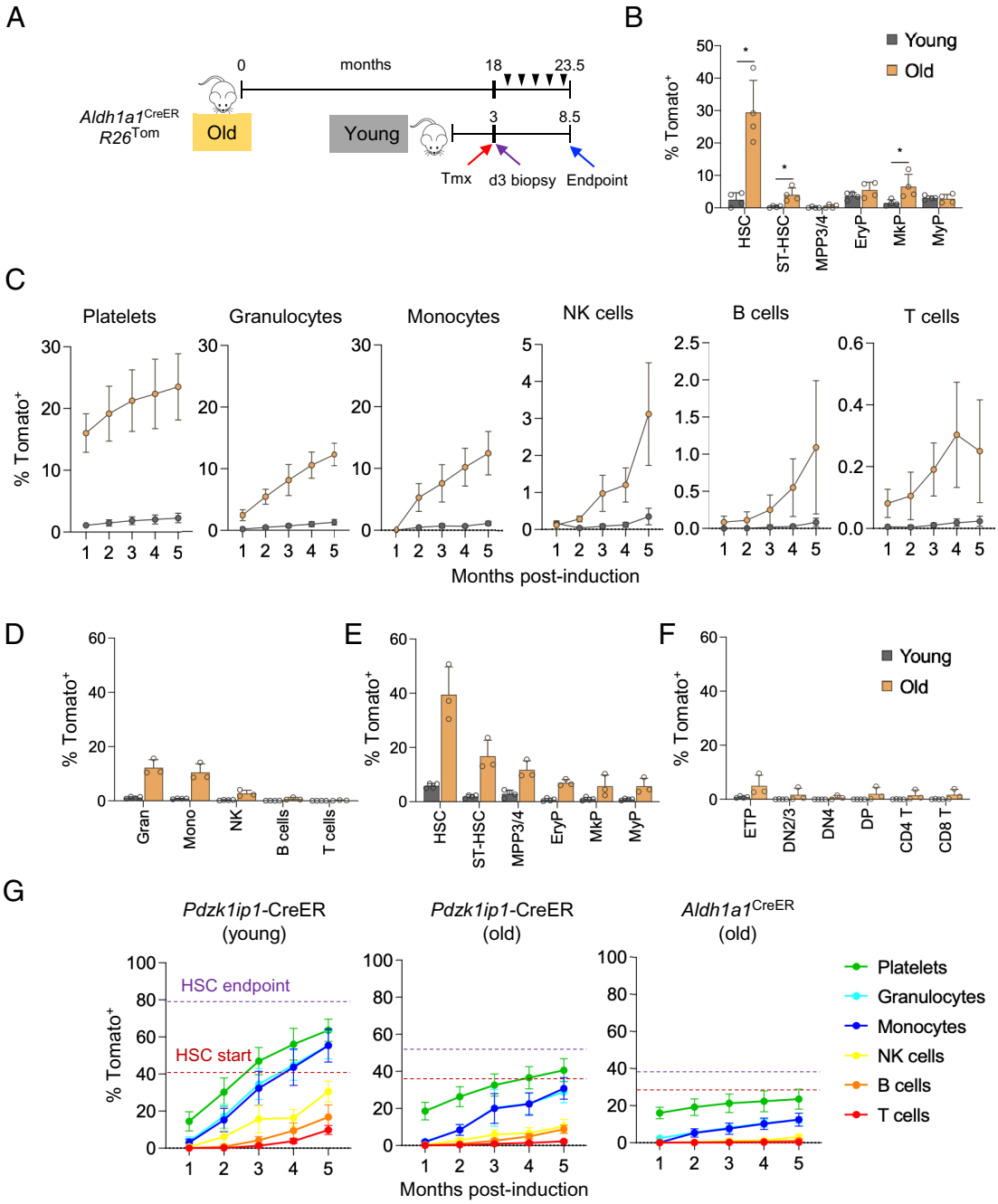

Fig. 4. Tracing endogenous HSCs using an aging-specific marker. (*A*) Labeling and long-term tracing of HSC using aging-specific *Aldh1a1*. *Aldh1a1*^{CreER} knockin mice were crossed with the Cre-inducible *Rosa26*-StopFlox-tdTomato (*R26*^{Tom}) fluorescent reporter. Old or young adult mice were treated with Tmx, examined by biopsy 3 d later, bled monthly (black arrowheads), and analyzed at the endpoint. (*B*) Fractions of Tom$^+$ cells within the indicated stem/progenitor cell types at 3 d. Symbols represent individual mice; bars represent mean ± SD. (*C*) Cell labeling in the peripheral blood of induced reporter animals. Shown are fractions of Tom$^+$ cells within the indicated cell type in young or old Tomato reporter mice at the indicated time points after tamoxifen induction. Symbols represent mean ± SD of 3 to 4 mice per group. (*D*–*F*) The analysis of reporter animals at the endpoint. Shown are fractions of labeled Tom$^+$ cells within mature cell types in the BM (*D*), stem/progenitor cells in the BM (*E*), and thymocyte subsets (*F*). Symbols represent individual mice; bars represent mean ± SD. (*G*) Comparison of labeling kinetics of the indicated cell types in the BM 5 mo postinduction in young (n = 3) or old (n = 7) *Pdzk1ip1*-CreER *R26*$^{Tom/Tom}$ mice or old *Aldh1a1*^{CreER} *R26*$^{Tom/Tom}$ reporter mice (n = 3). Data represent mean ± SD; dashed lines indicate average labeling of HSCs at the start and the endpoint of tracing. Statistical significance was estimated by Mann–Whitney *U* test. *$P < 0.05$.

lifetime. This is not consistent with the proposed view of HSCs as slowly differentiating "reserve" cells and confirms them as the primary active source of hematopoiesis (46). The notable exception was peripheral T cells, reflecting their maintenance via homeostatic proliferation (47). Furthermore, sublethal irradiation or exposure to IFN-I, whether acute or chronic, did not affect the rate or lineage spectrum of HSC-driven hematopoiesis. This observation differs from transplantation-based studies (22–24) and suggests that endogenous hematopoiesis is robust and resistant to major insults. On the contrary, aging was associated with reduced net contribution of HSCs to all hematopoietic lineages including platelets, myeloid cells, and lymphocytes. The reduction is even more pronounced when the numerical expansion of HSCs in old animals is taken into account. Importantly, our experiments do not rule out a stronger impairment of HSC-driven B and/or T cell development relative to other lineages, which may still

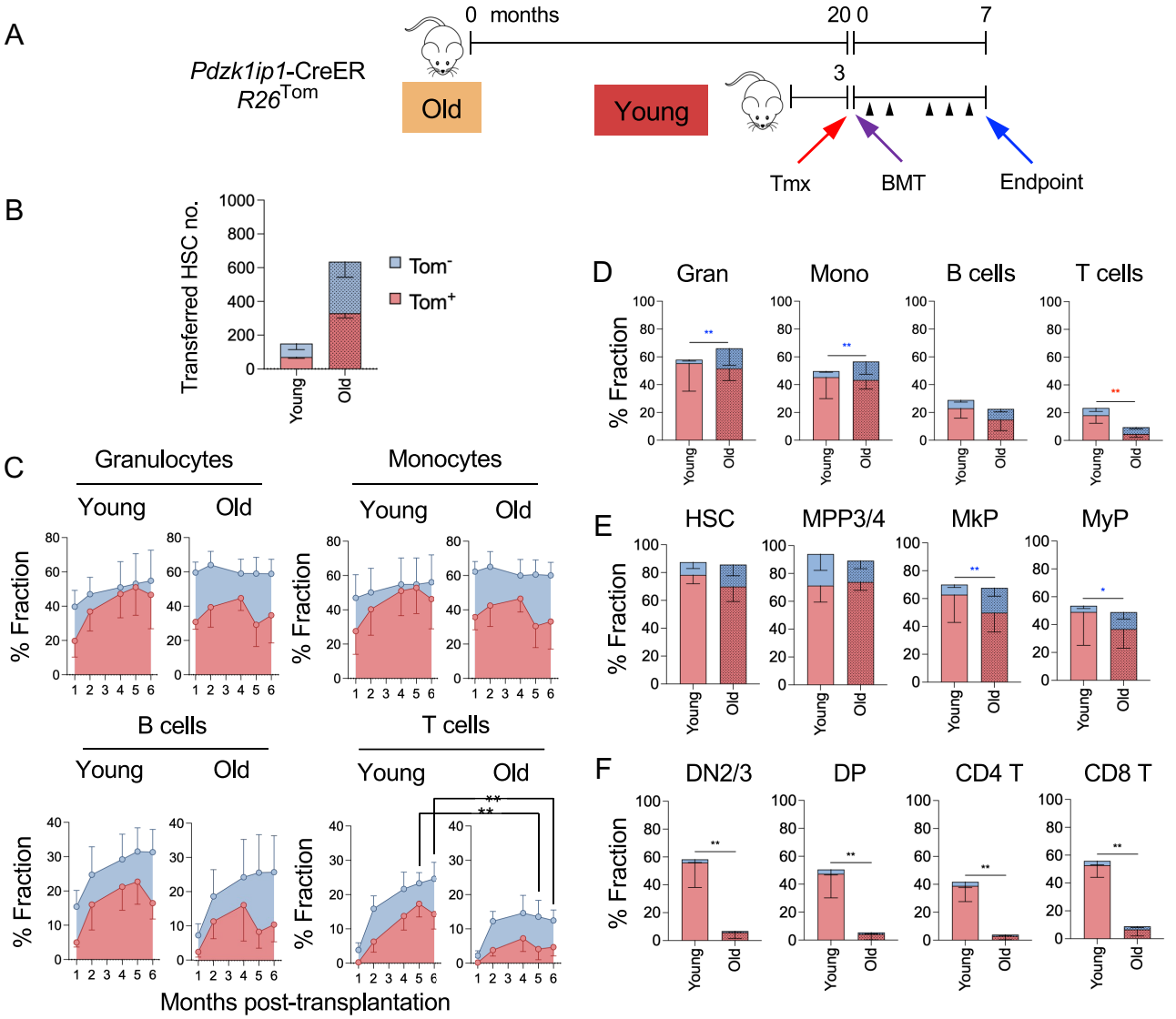

Fig. 5. Impaired contribution of aged HSC is compensated by other cell types. (*A*) Experimental design of BM transplantation with labeled HSCs. Old or young *Pdzk1ip1*-CreER R26$^{Tom/Tom}$ reporter mice were administered tamoxifen (Tmx) and killed 1 wk later. Total BM cells from these CD45.2 donor mice were mixed 1:1 with total BM cells from young CD45.1 congenic mice and transferred into lethally irradiated young CD45.1 congenic recipients. Two donor mice for each condition were induced, and donor cells from each animal were transferred separately. (*B*) The number of Tom$^+$ and Tom$^-$ HSCs in the total donor BM per recipient. Stacked bars represent mean of the respective values from 2 old or 2 young mice used as donors. (*C*) The analysis of donor-derived cells in the PB of recipient mice over time. Shown are fractions of CD45.2$^+$ Tom$^+$ cells (red) and Tom$^-$ cells (blue) in the indicated cell types of the recipients of young or old BM. Symbols represent mean ± SD of 6 or 5 recipients of old or young BM, respectively. Significant differences between total donor–derived cells in young vs. old BM recipients at 5 to 6 mo are indicated. (*D–F*) The analysis of recipient animals at the endpoint. Red, donor-derived Tom$^+$ cells; blue, donor-derived Tom$^-$ cells. Bars represent mean ± SD of the respective values from recipients of old (n = 6) or young (n = 5) BM. (*D*) The fraction of donor-derived cells in mature splenocytes. Significant differences in the fraction of Tom$^-$ cells (blue asterisks) or of Tom$^+$ cells (red asterisks) between young and old recipient groups are indicated. (*E*) The fraction of donor-derived cells in HSCs and progenitors in the BM. Significant differences in the fraction of Tom$^-$ cells (blue asterisks) between young and old recipient groups are indicated. (*F*) The fraction of donor-derived cells in thymocyte subsets. Significant differences in the fraction of Tom$^+$ cells between young and old recipient groups are indicated. Statistical significance was estimated by Mann–Whitney *U* test. *$P < 0.05$; **$P < 0.01$.

contribute to age-dependent decline of lymphopoiesis. Nevertheless, they establish a global reduction of multilineage HSC differentiation as a salient feature of hematopoiesis in old animals, which may represent a root cause of impaired lymphoid development and other age-associated defects.

The observed HSC decoupling is consistent with reduced HSC contribution to progenitors that was noted in old adult (11 to 16 mo old) compared to young (1 mo old) mice by lineage tracing (44). It also agrees with the reduced clonality of endogenous hematopoiesis in old mice (48) and humans (49), and with multiple functional and epigenetic defects of old HSCs such as impaired response to growth factors (50). On the contrary, it does not directly support the notion of myeloid bias, i.e., a normal or increased differentiation into myeloid and/or megakaryocytic lineages at the expense of lymphocytes. Such biases are well documented in transplantation settings, which measure HSC function in forced conditions of cell isolation, transfer, and hematopoietic reconstitution of heavily conditioned hosts. Indeed, transplantations with mild conditioning failed to reveal the myeloid bias in old HSCs (19). Thus, our results are compatible with the accumulation of myeloid- or platelet-biased HSCs in the old age; however, they did not reveal the net myeloid bias of the entire HSC population. Instead, they suggest that the regulated output of maturing blood cell precursors in older mice becomes decoupled from the differentiation potential of the HSCs from which they ultimately originate. The molecular basis of this age-associated decoupling remains to be elucidated but likely involves abnormalities of the old BM niche such as increased inflammatory cytokines

(51) and the concomitant decrease of important growth factors such as osteopontin (52), and/or specific intrinsic changes in older hematopoietic cells to growth factor responsiveness (50).

To probe the differentiation spectrum of old HSCs in an unbiased manner, we combined lineage tracing with single-cell transcriptomics, the combination that captures the dynamic "cutting edge" of differentiation on a real-time scale. The results from two time points (4 and 8 wk postlabeling) confirmed the comparable efficiency and time scale of HSC differentiation in young and old animals. Notably, this included the initial emergence of *Dntt*$^+$ progenitors with lymphoid potential (32), and the subsequent definitive lymphoid differentiation. We also used these data, supported by single-cell chromatin profiling, to analyze the HSC compartment itself. While some heterogeneity could be distinguished among HSCs as noted previously (53, 54), it was not substantially different between old and young HSCs. Moreover, the transcriptional and epigenetic signatures of old HSCs appeared evenly distributed among HSC subsets, including the expression of the lineage tracing marker *Aldh1a1*. Thus, the majority of HSCs appear to accumulate age-related transcriptional and epigenetic changes that underlie their decoupling from hematopoietic differentiation.

The transplantation experiments reported herein, in which we could distinguish the contribution of HSCs vs. other cells, showed that the defective function of old HSCs could be substituted by other sources in erythromyeloid but not in lymphoid cells. This was particularly prominent in T cell development, which showed a dramatic uncompensated reduction in these settings. This is consistent with a major compensatory capacity of hematopoiesis observed in HSC depletion experiments (55) and in genetic impairment of HSC function such as the deletion of Ikaros transcription factor, which abolishes lymphopoiesis but allows sufficient erythromyeloid development (56). The reduced differentiation of HSCs in old animals appears to be compensated from non-HSC sources, likely more differentiated stem/progenitor cells; however, the compensation is inefficient specifically in lymphopoiesis. The reasons for this remain to be elucidated, but likely reflect a distinct nature of lymphoid lineage commitment and differentiation. Indeed, lymphoid differentiation appears stochastic and relatively slow (29), and lymphoid progenitors are rare and quiescent by comparison to the abundant and proliferative erythromyeloid and megakaryocytic progenitors. In the case of T cell development, the lack of compensation may be exacerbated by the early differentiation stage of the would-be T cell precursor that exits the BM to seed the thymus (30, 57).

In conclusion, our study supports a model whereby hematopoiesis in the old age becomes quantitatively decoupled from the HSC population as its original source and becomes more reliant on more downstream progenitors. This transition compensates for impaired HSC activity in all lineages except lymphocytes, underlying the progressive decline of lymphopoiesis and of T cell development in particular. In addition to explaining the defective lymphopoiesis, this model has implications for other age-associated defects. For example, HSC decoupling may create selective pressure for mutations that confer advantage to HSC clones in myeloid differentiation and thereby promote ARCH and myeloproliferation. Future studies would test our model at the clonal level and help identify cell-intrinsic and cell-extrinsic factors that facilitate HSC decoupling in the old age.

Materials and Methods

Animals. All animal studies were performed according to the investigator's protocol approved by the Institutional Animal Care and Use Committee of New York University Grossman School of Medicine or by the French Ministry of Higher Education, Research and Innovation (APAFIS #32689-2021081015108361 v2) in accordance with European regulations. Wild-type C57BL/6 mice congenic for CD45.1 (B6.SJL-*Ptprc*^{a} *Pepc*^{b}/BoyCrl) were obtained from Charles River. *Pdzk1ip1*-CreER transgenic mouse strain and its cross to the Cre-inducible reporter strain *R26*$^{Tom/Tom}$ (B6;129S6-*Gt(ROSA)26Sor*$^{tm9(CAG-tdTomato)Hze}$/J) were described previously (21). *Aldh1a1*^{CreER} mice were described previously (40) and were crossed to *R26*^{Tom} mice.

Mice of both sexes were used in each experiment at the indicated ages. To induce Cre recombination, the mice were treated with the following doses of tamoxifen (Sigma-Aldrich) in sunflower oil by gavage: 1 mg (*Pdzk1ip1*-CreER *R26*$^{Tom/Tom}$) or 5 mg (*Aldh1a1*^{CreER} *R26*$^{Tom/Tom}$). The collection of PB (~0.1 mL) and BM biopsy (up to 20 µL of the BM/~10^6 cells) was performed as previously described (21). At the end point, animals were killed, and single-cell suspensions were prepared from the BM (femurs and tibiae), spleens, and thymi; counted; and analyzed by flow cytometry.

To induce proliferative stress, *Pdzk1ip1*-CreER *R26*$^{Tom/Tom}$ mice were sublethally irradiated (4.5 Gy) 7 wk prior to tamoxifen treatment. To induce acute interferon response, *Pdzk1ip1*-CreER *R26*$^{Tom/Tom}$ mice were injected i.p. with poly-I:C (100 mg, Invivogen) for three consecutive days 4 wk prior to tamoxifen treatment. To induce chronic interferon exposure, *Pdzk1ip1*-CreER *R26*$^{Tom/Tom}$ mice were injected i.v. with IFNα-Adv (Welgen) at 10^{10} virus particles/animal 10 wk prior to tamoxifen treatment.

Bone Marrow Transplantation. Old (20 mo) or control adult (3 mo) *Pdzk1ip1*-CreER *R26*$^{Tom/Tom}$ mice were administered with tamoxifen. After 7 d, total BM cells were isolated, mixed 1:1 with total BM cells from CD45.1 congenic mice, and transferred into lethally irradiated CD45.1 congenic recipients at 10^6 total cells/recipient. BM cells from two donor mice were prepared and transferred separately into two groups of recipients. Labeled HSC-derived cells in the recipient mice were defined as CD45.1$^-$ CD45.2$^+$ Tom$^+$ cells; total donor-derived cells were defined as CD45.1$^-$ CD45.2$^+$ (Tom$^+$ or Tom$^-$).

Cell Staining and Flow Cytometry. Cells from peripheral blood, BM, spleens, and thymi were subjected to red blood cell lysis, washed, and suspended in PBS containing 2% fetal bovine serum (FBS). The cells were stained with the fluorochrome-conjugated antibodies for 20 to 60 min in 2% FBS containing PBS. Samples were acquired on an Attune NxT flow cytometer (Thermo Fisher Scientific) and analyzed using FlowJo software (FlowJo, LLC). Cell populations were defined as described before (21) and specified in *SI Appendix, Methods*.

CITE-Seq. Old (20 mo) and young (3 mo) *Pdzk1ip1*-CreER *R26*$^{Tom/Tom}$ mice were treated with 0.5 mg tamoxifen in sunflower oil administered by gavage. To assess specificity of the labeling, cells were obtained by BM biopsy at 3 d postinduction and analyzed using flow cytometry. After 4- or 8-wk postinduction, mice were killed, and femur, tibia, humerus, and pelvis were collected. Bones were crushed in the presence of PBS with 2% FBS, and muscle and bone material were removed with a 40-µm strainer. Red blood cells were removed with red blood cell lysis buffer, washed, and stained with Fc blocker (BioLegend). Lineage cells were depleted with the Streptavidin Microbead kit (Miltenyi) using two different cocktails of biotinylated antibodies according to each time point. For the 4-wk timepoint, we used Gr-1, CD19, TCRb, Ter119, CD11b, and NK1.1 and for the 8-wk timepoint, we used Gr-1, CD19, TCRb, and Ter119. After lineage depletion, cells from each animal were stained separately with the dead cell dye Zombie Aqua (BioLegend), followed by incubation with Pacific Blue-conjugated lineage antibodies, unique hashtags, as well as a cocktail of 25 different TotalSeq-A antibodies (BioLegend). In order to use the same antibody for both cell sorting and CITE-Seq analysis, the TotalSeq-A antibodies against CD117 and CD135 were conjugated to AlexaFluor 647 fluorophore (/5Alex647N/$(T)_{30}$, IDT) and used at 4-wk and 8-wk time points, respectively. After staining and three washing steps to remove unbound TotalSeq-A antibodies, Lin$^-$ cKit$^+$ Tom$^+$ (at 4 wk) or Lin$^-$ Flt3$^+$ Tom$^+$ (at 8 wk) cells were sorted and collected in PBS with 1% BSA. Equivalent numbers of sorted cell from each animal were mixed, and the resulting cell mixture was prepared according to 10× Genomics protocol and loaded onto the 10× Chromium Controller for GEM generation and barcoding. Sequencing and analysis were done as described in *SI Appendix, Methods*.

Statistical Analysis. Statistical significance was determined by nonparametric Mann–Whitney test using the Prism software (GraphPad).

Data, Materials, and Software Availability. CITE-Seq data have been deposited in the Gene Expression Omnibus database of the National Center for Biotechnology Information under accession number GSE229018 (58).

ACKNOWLEDGMENTS. We acknowledge the use of New York University Genome Technology Center, which is partially supported by the Laura and Isaac Perlmutter Cancer Center. This study was supported by the NIH grants AG049074 and HL152637 (B.R.); Edward P. Evans Foundation (B.R.); Damon Runyon Postdoctoral Fellowship DRG 2408-20 (N.M.A.); New York State Stem Cell Science training grant (G.J.); Action thématique incitative sur programme-Avenir award (C.M.S.); European Hematology Association Advanced Research Award (C.M.S.); and Institut National du Cancer grant 2018-143 (C.M.S.).

Author affiliations: [a]Department of Pathology, New York University Grossman School of Medicine, New York, NY 10016; [b]INSERM Unit 1312 Bordeaux Institute of Oncology, University of Bordeaux 33076 Bordeaux, France; [c]Applied Bioinformatics Laboratories, New York University Grossman School of Medicine, New York, NY 10016; and [d]Department of Neurology, Feinberg School of Medicine, Northwestern University, Chicago, IL 60611

1. H. W. Snoeck, Aging of the hematopoietic system. *Curr. Opin. Hematol.* **20**, 355–361 (2013).
2. R. J. Lin, H. K. Elias, M. R. van den Brink, Immune reconstitution in the aging host: Opportunities for mechanism-based therapy in allogeneic hematopoietic cell transplantation. *Front. Immunol.* **12**, 674093 (2021).
3. E. V. Verovskaya, P. V. Dellorusso, E. Passegue, Losing sense of self and surroundings: Hematopoietic stem cell aging and leukemic transformation. *Trends Mol. Med.* **25**, 494–515 (2019).
4. C. J. Eaves, Hematopoietic stem cells: Concepts, definitions, and the new reality. *Blood* **125**, 2605–2613 (2015).
5. E. Laurenti, B. Gottgens, From haematopoietic stem cells to complex differentiation landscapes. *Nature* **553**, 418–426 (2018).
6. G. de Haan, S. S. Lazare, Aging of hematopoietic stem cells. *Blood* **131**, 479–487 (2018).
7. C. E. Muller-Sieburg, R. H. Cho, L. Karlsson, J. F. Huang, H. B. Sieburg, Myeloid-biased hematopoietic stem cells have extensive self-renewal capacity but generate diminished lymphoid progeny with impaired IL-7 responsiveness. *Blood* **103**, 4111–4118 (2004).
8. B. Dykstra *et al.*, Long-term propagation of distinct hematopoietic differentiation programs in vivo. *Cell Stem Cell* **1**, 218–229 (2007).
9. G. A. Challen, N. C. Boles, S. M. Chambers, M. A. Goodell, Distinct hematopoietic stem cell subtypes are differentially regulated by TGF-beta1. *Cell Stem Cell* **6**, 265–278 (2010).
10. Y. Morita, H. Ema, H. Nakauchi, Heterogeneity and hierarchy within the most primitive hematopoietic stem cell compartment. *J. Exp. Med.* **207**, 1173–1182 (2010).
11. J. Carrelha *et al.*, Hierarchically related lineage-restricted fates of multipotent haematopoietic stem cells. *Nature* **554**, 106–111 (2018).
12. R. H. Cho, H. B. Sieburg, C. E. Muller-Sieburg, A new mechanism for the aging of hematopoietic stem cells: Aging changes the clonal composition of the stem cell compartment but not individual stem cells. *Blood* **111**, 5553–5561 (2008).
13. I. Beerman *et al.*, Functionally distinct hematopoietic stem cells modulate hematopoietic lineage potential during aging by a mechanism of clonal expansion. *Proc. Natl. Acad. Sci. U.S.A.* **107**, 5465–5470 (2010).
14. K. Sudo, H. Ema, Y. Morita, H. Nakauchi, Age-associated characteristics of murine hematopoietic stem cells. *J. Exp. Med.* **192**, 1273–1280 (2000).
15. S. M. Chambers *et al.*, Aging hematopoietic stem cells decline in function and exhibit epigenetic dysregulation. *PLoS Biol.* **5**, e201 (2007).
16. B. Dykstra, S. Olthof, J. Schreuder, M. Ritsema, G. de Haan, Clonal analysis reveals multiple functional defects of aged murine hematopoietic stem cells. *J. Exp. Med.* **208**, 2691–2703 (2011).
17. H. Leins *et al.*, Aged murine hematopoietic stem cells drive aging-associated immune remodeling. *Blood* **132**, 565–576 (2018).
18. W. Kuribayashi *et al.*, Limited rejuvenation of aged hematopoietic stem cells in young bone marrow niche. *J. Exp. Med.* **218**, e20192283 (2021).
19. E. Montecino-Rodriguez *et al.*, Lymphoid-biased hematopoietic stem cells are maintained with age and efficiently generate lymphoid progeny. *Stem Cell Reports* **12**, 584–596 (2019).
20. Y. Liang, G. Van Zant, S. J. Szilvassy, Effects of aging on the homing and engraftment of murine hematopoietic stem and progenitor cells. *Blood* **106**, 1479–1487 (2005).
21. C. M. Sawai *et al.*, Hematopoietic stem cells are the major source of multilineage hematopoiesis in adult animals. *Immunity* **45**, 597–609 (2016).
22. M. A. Essers *et al.*, IFNalpha activates dormant haematopoietic stem cells in vivo. *Nature* **458**, 904–908 (2009).
23. E. M. Pietras *et al.*, Re-entry into quiescence protects hematopoietic stem cells from the killing effect of chronic exposure to type I interferons. *J. Exp. Med.* **211**, 245–262 (2014).
24. D. Walter *et al.*, Exit from dormancy provokes DNA-damage-induced attrition in haematopoietic stem cells. *Nature* **520**, 549–552 (2015).
25. A. Mathian, A. Weinberg, M. Gallegos, J. Banchereau, S. Koutouzov, IFN-alpha induces early lethal lupus in preautoimmune (New Zealand Black x New Zealand White) F1 but not in BALB/c mice. *J. Immunol.* **174**, 2499–2506 (2005).
26. M. Stoeckius *et al.*, Simultaneous epitope and transcriptome measurement in single cells. *Nat. Methods* **14**, 865–868 (2017).
27. M. Stoeckius *et al.*, Cell Hashing with barcoded antibodies enables multiplexing and doublet detection for single cell genomics. *Genome Biol.* **19**, 224 (2018).
28. A. Flohr Svendsen *et al.*, A comprehensive transcriptome signature of murine hematopoietic stem cell aging. *Blood* **138**, 439–451 (2021).
29. S. Upadhaya *et al.*, Kinetics of adult hematopoietic stem cell differentiation in vivo. *J. Exp. Med.* **215**, 2815–2832 (2018).
30. E. L. Y. Chen, P. K. Thompson, J. C. Zuniga-Pflucker, RBPJ-dependent Notch signaling initiates the T cell program in a subset of thymus-seeding progenitors. *Nat. Immunol.* **20**, 1456–1468 (2019).
31. D. Amann-Zalcenstein *et al.*, A new lymphoid-primed progenitor marked by Dach1 downregulation identified with single cell multi-omics. *Nat. Immunol.* **21**, 1574–1584 (2020).
32. F. Klein *et al.*, Dntt expression reveals developmental hierarchy and lineage specification of hematopoietic progenitors. *Nat. Immunol.* **23**, 505–517 (2022).
33. J. Feng *et al.*, Clonal lineage tracing reveals shared origin of conventional and plasmacytoid dendritic cells. *Immunity* **55**, 405–422.e11 (2022).
34. D. A. Sultana, J. J. Bell, D. A. Zlotoff, M. E. De Obaldia, A. Bhandoola, Eliciting the T cell fate with Notch. *Semin Immunol.* **22**, 254–260 (2010).
35. D. A. Zlotoff *et al.*, CCR7 and CCR9 together recruit hematopoietic progenitors to the adult thymus. *Blood* **115**, 1897–1905 (2010).
36. H. Yoshida *et al.*, The cis-regulatory atlas of the mouse immune system. *Cell* **176**, 897–912.e20 (2019).
37. N. Itokawa *et al.*, Epigenetic traits inscribed in chromatin accessibility in aged hematopoietic stem cells. *Nat. Commun.* **13**, 2691 (2022).
38. B. P. Levi, O. H. Yilmaz, G. Duester, S. J. Morrison, Aldehyde dehydrogenase 1a1 is dispensable for stem cell function in the mouse hematopoietic and nervous systems. *Blood* **113**, 1670–1680 (2009).
39. A. Grover *et al.*, Single-cell RNA sequencing reveals molecular and functional platelet bias of aged haematopoietic stem cells. *Nat. Commun.* **7**, 11075 (2016).
40. J. F. Poulin *et al.*, Mapping projections of molecularly defined dopamine neuron subtypes using intersectional genetic approaches. *Nat. Neurosci.* **21**, 1260–1271 (2018).
41. A. Sanchez-Aguilera *et al.*, Estrogen signaling selectively induces apoptosis of hematopoietic progenitors and myeloid neoplasms without harming steady-state hematopoiesis. *Cell Stem Cell* **15**, 791–804 (2014).
42. K. L. Medina *et al.*, Identification of very early lymphoid precursors in bone marrow and their regulation by estrogen. *Nat. Immunol.* **2**, 718–724 (2001).
43. K. Busch *et al.*, Fundamental properties of unperturbed haematopoiesis from stem cells in vivo. *Nature* **518**, 542–546 (2015).
44. P. Sawen *et al.*, Murine HSCs contribute actively to native hematopoiesis but with reduced differentiation capacity upon aging. *Elife* **7**, e41258 (2018).
45. R. H. Chapple *et al.*, Lineage tracing of murine adult hematopoietic stem cells reveals active contribution to steady-state hematopoiesis. *Blood Adv.* **2**, 1220–1228 (2018).
46. J. N. Pucella, S. Upadhaya, B. Reizis, The source and dynamics of adult hematopoiesis: Insights from lineage tracing. *Annu. Rev. Cell Dev. Biol.* **36**, 529–550 (2020).
47. J. Sprent, C. D. Surh, Normal T cell homeostasis: The conversion of naive cells into memory-phenotype cells. *Nat. Immunol.* **12**, 478–484 (2011).
48. M. Ganuza *et al.*, The global clonal complexity of the murine blood system declines throughout life and after serial transplantation. *Blood* **133**, 1927–1942 (2019).
49. E. Mitchell *et al.*, Clonal dynamics of haematopoiesis across the human lifespan. *Nature* **606**, 343–350 (2022).
50. C. A. Hammond, S. W. Wu, F. Wang, M. E. MacAldaz, C. J. Eaves, Aging alters the cell cycle control and mitogenic signaling responses of human hematopoietic stem cells. *Blood* **141**, 1990–2002 (2023), 10.1182/blood.2022017174.
51. C. A. Mitchell *et al.*, Stromal niche inflammation mediated by IL-1 signalling is a targetable driver of haematopoietic ageing. *Nat. Cell Biol.* **25**, 30–41 (2023).
52. N. Guidi *et al.*, Osteopontin attenuates aging-associated phenotypes of hematopoietic stem cells. *EMBO J.* **36**, 840–853 (2017).
53. M. S. Kowalczyk *et al.*, Single-cell RNA-seq reveals changes in cell cycle and differentiation programs upon aging of hematopoietic stem cells. *Genome Res.* **25**, 1860–1872 (2015).
54. E. M. Fast *et al.*, External signals regulate continuous transcriptional states in hematopoietic stem cells. *Elife* **10**, e66512 (2021).
55. K. B. Schoedel *et al.*, The bulk of the hematopoietic stem cell population is dispensable for murine steady-state and stress hematopoiesis. *Blood* **128**, 2285–2296 (2016).
56. A. Nichogiannopoulou, M. Trevisan, S. Neben, C. Friedrich, K. Georgopoulos, Defects in hemopoietic stem cell activity in Ikaros mutant mice. *J. Exp. Med.* **190**, 1201–1214 (1999).
57. B. A. Schwarz *et al.*, Selective thymus settling regulated by cytokine and chemokine receptors. *J. Immunol.* **178**, 2008–2017 (2007).
58. G. Jang, S. Contreras Castillo, E. Esteva, C. M. Sawai, B. Reizis, Single *cell* transcriptomic and chromatin accessibility profiling of hematopoietic *stem cells* and progenitors during *aging*. *Gene Expression Omnibus*. https://www.ncbi.nlm.nih.gov/geo/query/acc.cgi?acc=GSE229018. Deposited 5 April 2023.